

Supporting Information

Efficient full solar spectrum-driven photocatalytic hydrogen production on low bandgap TiO₂/conjugated polymer nanostructures.

Edith Mawunya Kutorglo^{1,2,*}, Michael Schwarze¹, Anh Dung Nguyen¹, Simon Tameu Djoko¹, Shahana Huseyinova^{1,3}, Minoo Tasbihi¹, Oliver Görke⁴, Matthias Primbs⁵, Miroslav Šoóš², Reinhard Schomäcker¹

¹Department of Chemistry, Technische Universität Berlin, Straße des 17. Juni 124, TC8, 10623 Berlin, Germany.

²Bioengineering and Advanced Materials Laboratory, Department of Chemical Engineering, University of Chemistry and Technology Prague, 166 28 Prague, Czech Republic.

³University of Santiago de Compostela, Department of Chemistry, Avenida do Mestre Mateo 25, 15706 Santiago de Compostela, Spain

⁴Department of Ceramic Materials, Faculty III: Process Sciences, Technische Universität Berlin, 10623 Berlin, Germany.

⁵The Electrochemical Energy, Catalysis, and Materials Science Laboratory, Department of Chemistry, Chemical Engineering Division, Technische Universität Berlin, 10623 Berlin, Germany.

Table of Contents

| | <u>Content</u> | <u>Page</u> |
|----|-----------------------------------------------------------------------------------------------------------------------------------------------------------------------------------------------------------------------------|-------------|
| 1. | Figure SI 1. Setup for the H ₂ production tests | 2 |
| 2. | Figure SI 2. Effect of PVA concentration on BET surface area of m-TiO ₂ and (b) effect of hydrolysis temperature on the crystalline properties of TiO ₂ | 3 |
| 3. | Figure SI 3. Effect of calcination temperature on BET surface area of m-TiO ₂ and (b) effect of hydrolysis temperature on the crystalline properties of m-TiO ₂ | 4 |
| 4. | Text S1. Selecting optimum calcination conditions | 5 |
| 5. | Figure SI 4 Influence of calcination temperature on H ₂ production and BET surface area of m-TiO ₂ | 6 |
| 6. | Figure SI 5 N ₂ adsorption-desorption isotherm of TiO ₂ before and after calcination | 7 |
| 7. | Figure SI 6 SEM images showing sintering effect of TiO ₂ calcined at different temperatures. Table S1 summarizing the effect of calcination temperature on H ₂ production and textural properties. | 8 |
| 8. | Fig. SI 7 EDX spectra confirming the presence of Pt NPs on m-TiO ₂ | 9 |
| 9. | Fig. SI 8 Control experiment using Pt NPs only with irradiation under solar simulation | 10 |

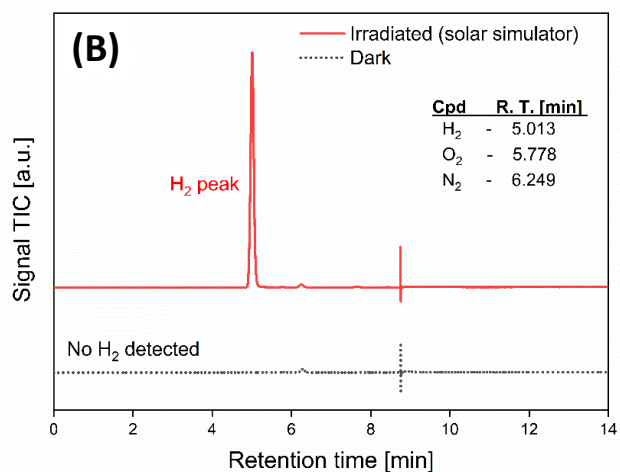
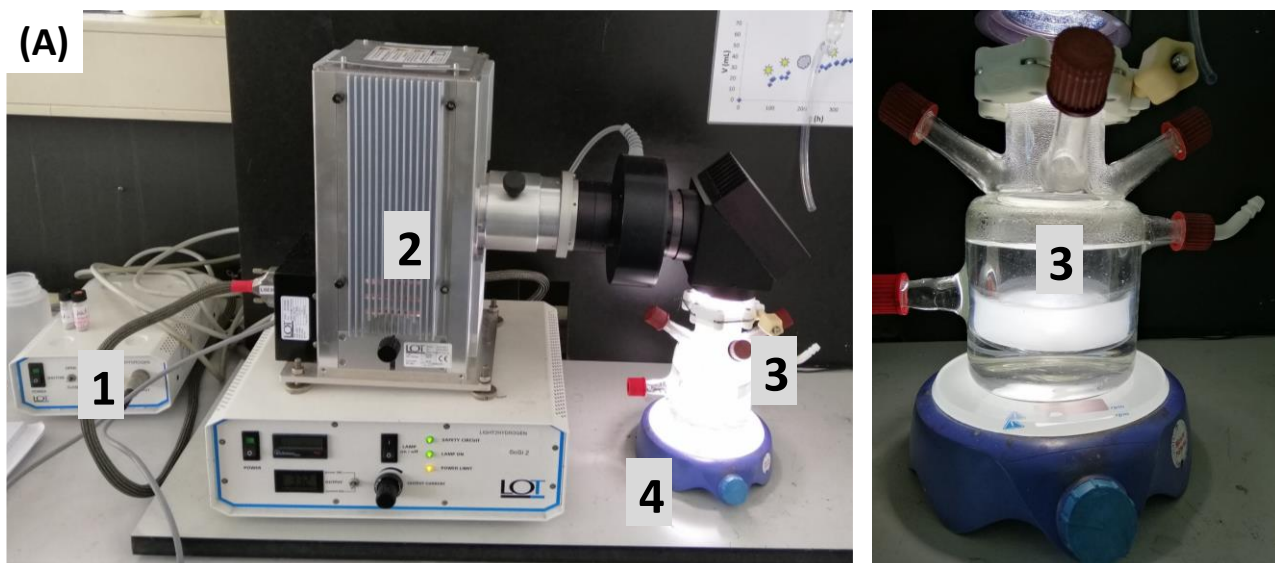


Figure SI 1. A) Setup for the H₂ production tests: (1) Filter, (2) solar simulator (300 W Xe lamp with AM 1.5 filter), (3) top irradiation photoreactor, and (4) magnetic stirrer. B) A gas chromatograph for a collected sample of generated hydrogen stream under a solar simulator.

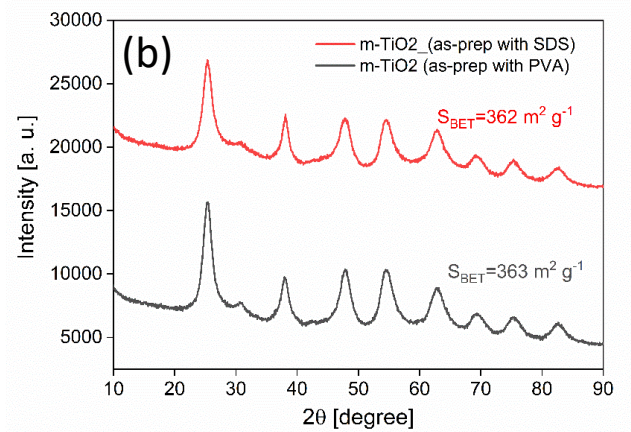
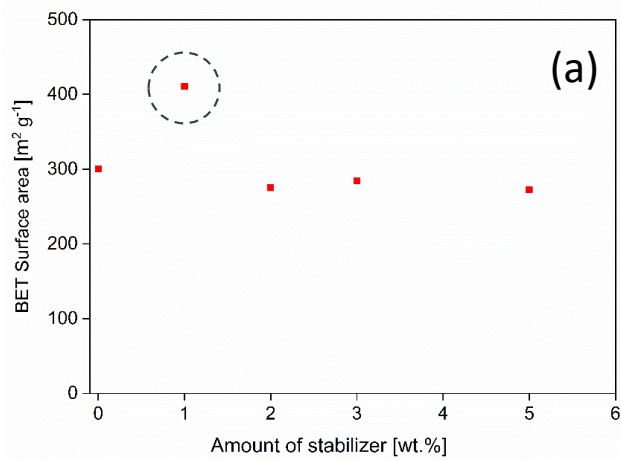


Figure SI 2. (a) Influence of stabilizer amount on BET surface area of m-TiO₂ and (b) XRD pattern for m-TiO₂ prepared with PVA or SDS.

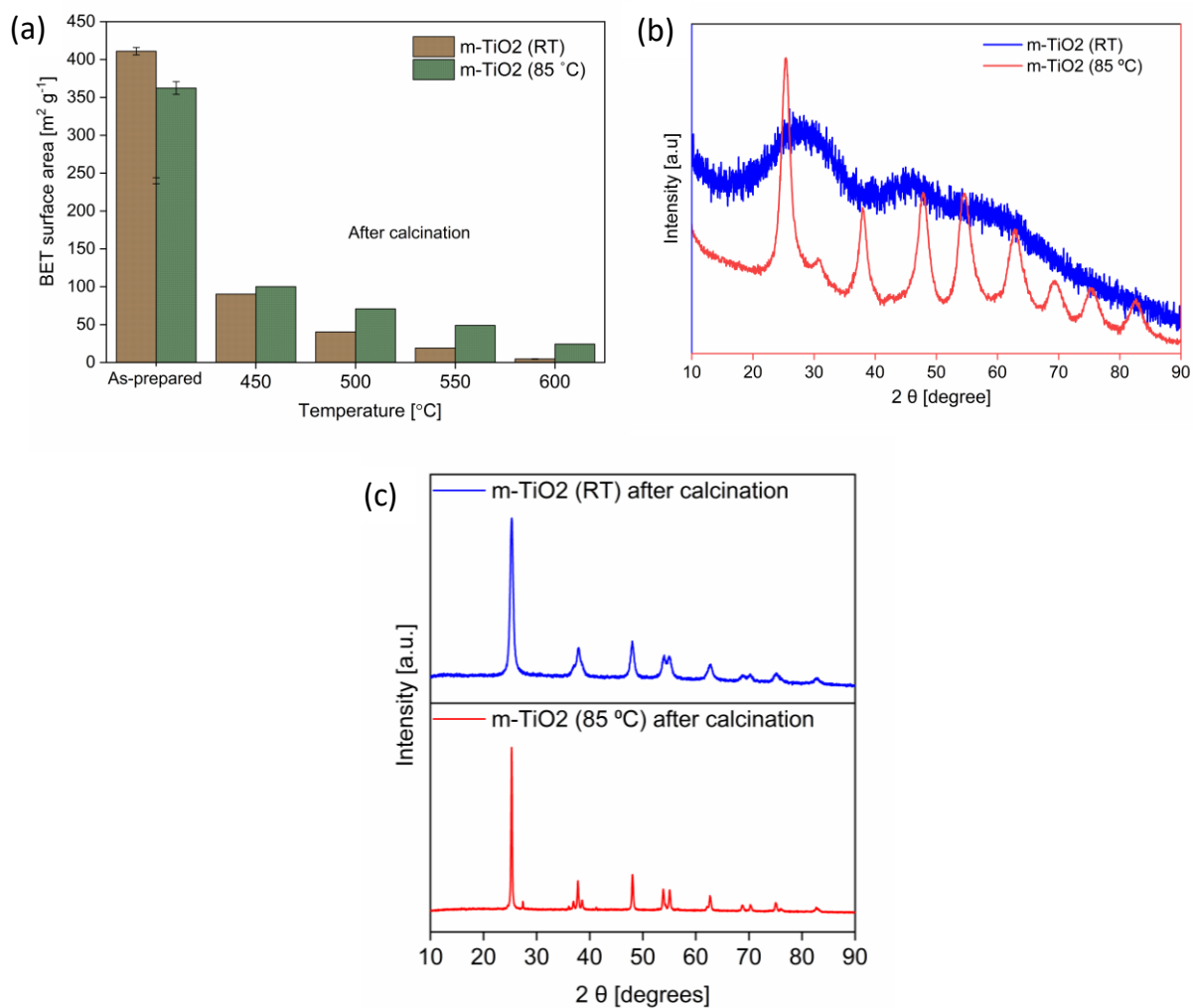


Figure SI 3. (a) Effect of calcination temperature on BET surface area of m-TiO₂ and (b) effect of hydrolysis temperature on the crystalline properties of m-TiO₂ (c) catalysts after calcination

The XRD pattern of the as-prepared catalysts (Figure SI 3 (b)) confirmed that m-TiO₂ prepared at 85 °C was crystalline, whereas TiO₂ prepared at 25 °C was amorphous and was only converted to crystalline upon subsequent calcination treatment (Figure SI 3 (c)).

Text S1: Selecting the Optimum calcination conditions

The performance of any given material is dependent on its physicochemical properties, which are determined by the preparation conditions. Although high-temperature treatment in air has been reported to result in crystallization which leads to enhanced photocatalytic activity, calcination is also known to induce sintering and aggregation of the catalyst particles which can compromise the photocatalytic activity[1]. In view of this, we performed calcinations at different temperatures and evaluated the optimal temperature at which the surface area and crystalline properties were preserved and the highest amount of hydrogen was produced. The as-prepared m-TiO₂ exhibited a reasonably good hydrogen evolution activity of 1.36 mmol g⁻¹ h⁻¹ under simulated sunlight conditions. Increasing the calcination temperature from 200 to 400 °C did not affect the H₂ production compared to the as-prepared material (Figure SI 4, Table SI 1 below). Above this temperature, the rate of hydrogen production increased. Mesoporous TiO₂ nanostructures calcined at 550 °C for 3 h in air showed the highest H₂ production rate. A further increase in the calcination temperature from 550 to 600 °C resulted in a decrease in the hydrogen production rate from 5.34 to 4.24 mmol g⁻¹ h⁻¹, which also corresponded to a significant decrease in the surface area from 49 m²g⁻¹ to 24 m²g⁻¹. This could be attributed to increased interparticle contact and a high degree of sintering of the particles at high temperatures as confirmed by SEM images and a broader pore size distribution (Figure SI 5 and 6, respectively below). These observations are in agreement with other studies which reported a high degree of sintering of catalyst particles at temperatures higher than 600 °C [2]. Miszczak and Pietrzyk [3] have also reported that anatase to rutile phase transition occurs at temperatures above 600 °C which decreases the photocatalytic activity. Overall, these results suggest that heat treatment of m-TiO₂ with temperatures between 450 °C and 550 °C has a positive impact on the photocatalytic H₂ production performance.

Apart from the calcination temperature, the calcination atmosphere also significantly influences the textural properties and photocatalytic activity of the catalysts. When the optimum material m-TiO₂ was calcined under N₂ atmosphere instead of air, the BET surface area increased (See Table SI 1, Entry 9 and 10) but the H₂ production rate decreased to about half. Considering the higher surface area, the decrease in activity could be due to changes in the crystal structure, which was also evident from a color change from white to black (See Scheme 1 (c) in the main text). In addition, the color change also indicates changes in the oxidation states of TiO₂ in an oxygen-deficient environment. Therefore, the surface area is not the main factor determining photocatalytic activity. Evidently, the activity is based on a combination of optimal surface area, absorption, and crystalline properties. In the case of the hybrid m-TiO₂/PPy nanostructures, a similar trend was observed upon calcination with the optimum material obtained after calcination at 550 °C for 3 h in air. Nonetheless, the H₂ production rate of the calcined TiO₂-PPy composite material increased only slightly after calcination (from 1.58 to 1.95 mmol g⁻¹h⁻¹) compared to that of the m-TiO₂, whose activity increased about 4 times after calcination in air (1.36 to 5.34 mmol g⁻¹ h⁻¹). The lower photocatalytic activity of the composites after the calcination could be due to the instability of PPy under the calcination conditions (550 °C, air), which is in line with previous reports [4]. These results are summarized in Table S1, below. To test whether the degradation of PPy can be prevented, m-TiO₂/PPy was calcined under an N₂ atmosphere. Similar to the observation with pure m-TiO₂, the m-TiO₂/PPy calcined under an N₂ atmosphere turned black in color, and its activity was reduced by half (Table S1, Entries 16 in Supporting Information). In the future, we plan to investigate photosensitizers with higher thermal stability such as porphyrins or metal phthalocyanines.

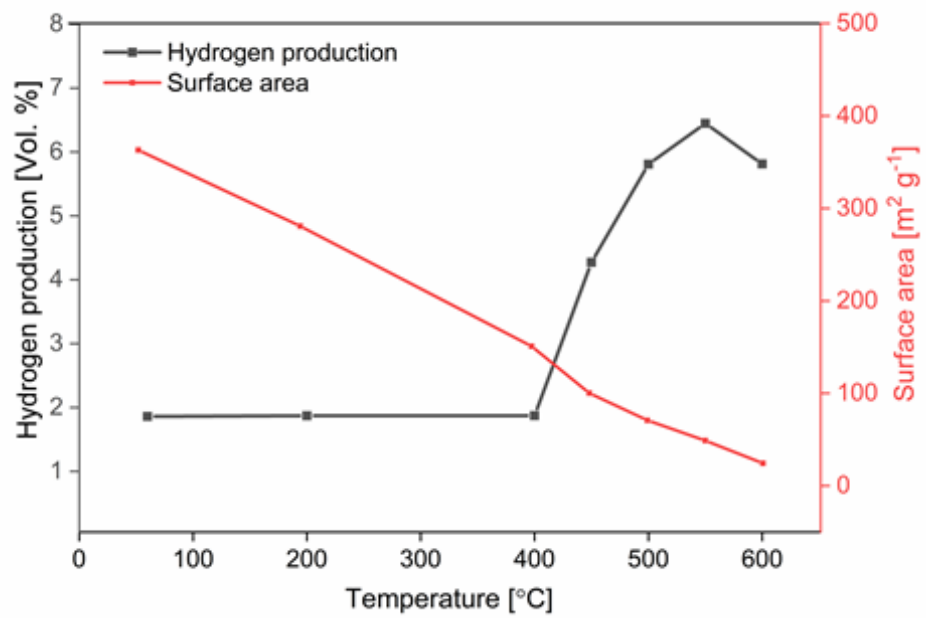


Figure SI 4. Influence of calcination temperature on H₂ production and BET surface area of m-TiO₂.

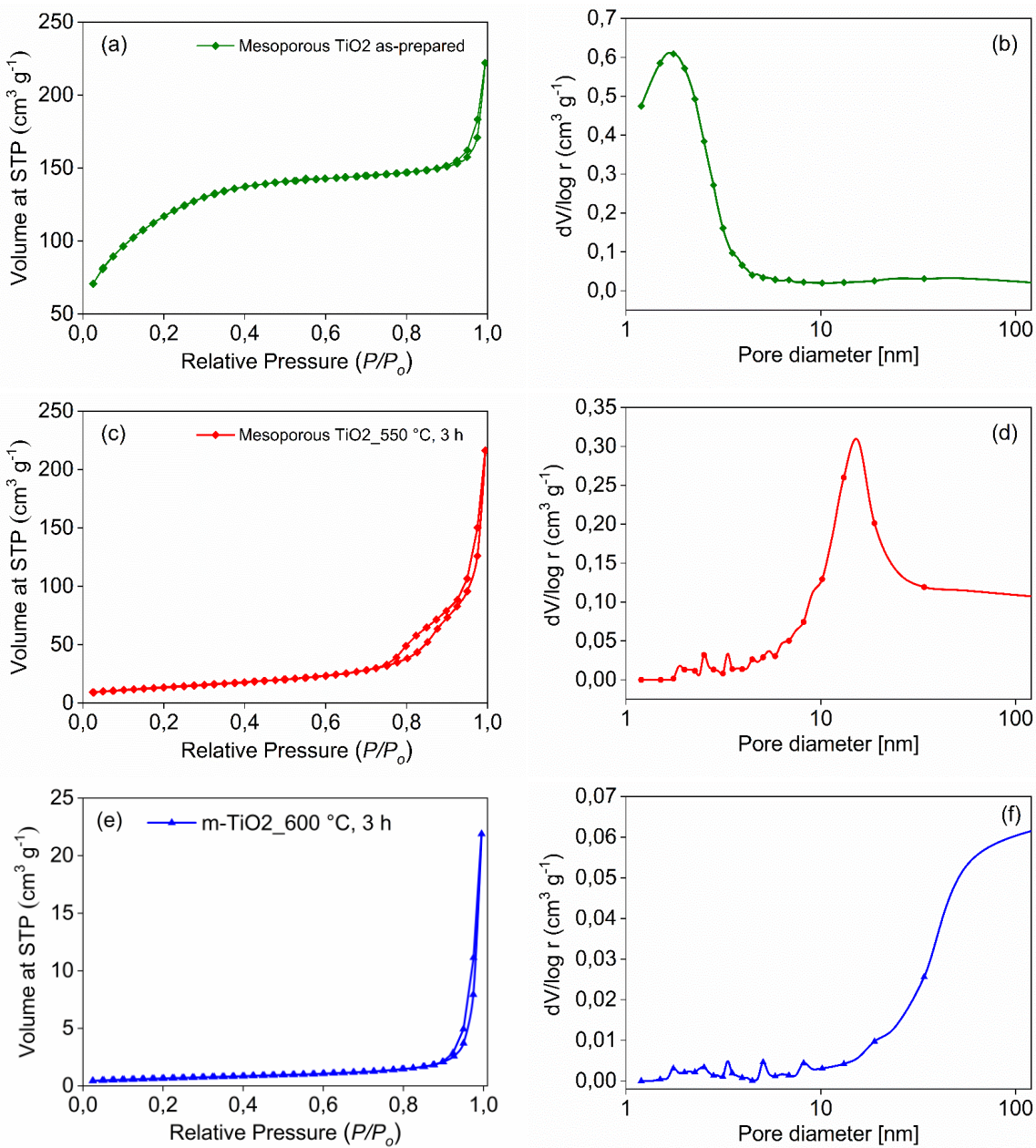


Figure SI 5. N₂ adsorption-desorption isotherm of (a) as-prepared m-TiO₂, (c) m-TiO₂ calcined for 3h at 550 °C, (e) m-TiO₂ calcined for 3h at 600 °C, and their corresponding pore size distributions (b), (d) and (f).

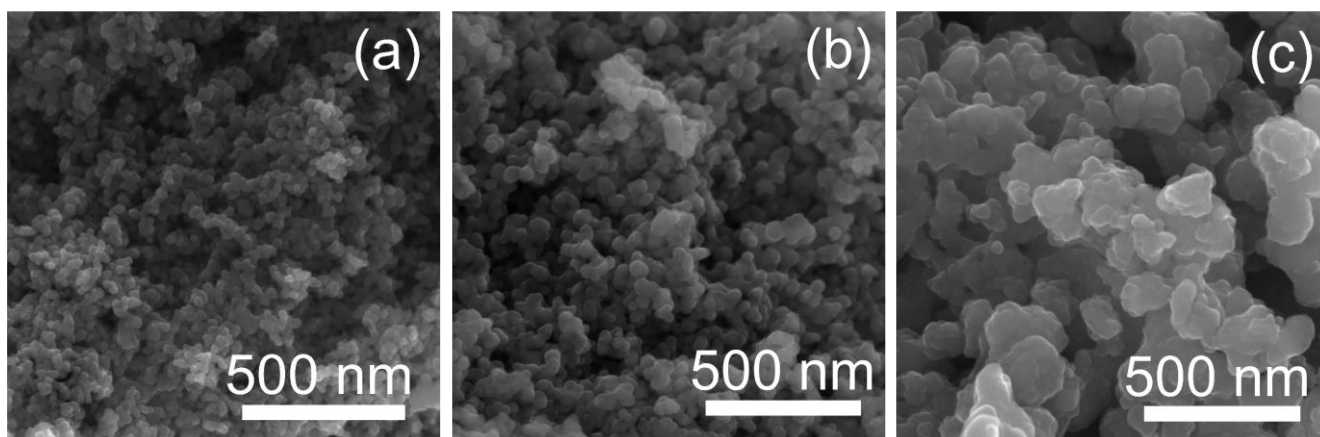


Figure SI 6. Sintering effect of TiO₂ calcined at different temperatures (a) as-prepared, (b) calcined at 550 °C, and (c) calcined at 600 °C.

Table SI 1. Effect of calcination temperature on H₂ production and textural properties, calcination was performed in air in all cases for 3 hours. m-TiO₂ (RT) and m-TiO₂ (HT) refer to mesoporous TiO₂ where hydrolysis was performed at room temperature and 85 °C, respectively.

| | Sample | Calcination Temperature [°C] | BET Surface Area [m ² g ⁻¹] | H ₂ production [mmol g ⁻¹ h ⁻¹] |
|-----|-------------------------------------------------------|------------------------------|----------------------------------------------------|-------------------------------------------------------------------|
| 1. | m-TiO ₂ (RT) as-prepared | 60 | 411 | 1.36 |
| 2. | m-TiO ₂ (RT)_450 | 450 | 90 | 2.77 |
| 3. | m-TiO ₂ (RT)_500 | 500 | 40 | 2.89 |
| 4. | m-TiO ₂ (RT)_550 | 550 | 21 | 3.24 |
| 5. | m-TiO ₂ (RT)_600 | 600 | 5 | 1.31 |
| 6. | m-TiO ₂ (HT) as-prepared | 60 | 363 | 1.36 |
| 7. | m-TiO ₂ (HT)_450 | 450 | 100 | 4.24 |
| 8. | m-TiO ₂ (HT)_500 | 500 | 71 | 4.49 |
| 9. | m-TiO ₂ (HT)_550 in air | 550 | 49 | 5.34 |
| 10. | m-TiO₂ (HT)_550 under N₂ | 550 | 123 | 2.13 |
| 11. | m-TiO ₂ (HT)_600 | 600 | 24 | 4.24 |
| 12. | TiO ₂ -PPy_as-prepared | 60 | 237 | 1.58 |
| 13. | TiO ₂ -PPy_450 | 450 | 144 | 1.62 |
| 14. | TiO ₂ -PPy_500 | 500 | 106 | 1.77 |
| 15. | TiO ₂ -PPy_550 in air | 550 | 105 | 1.95 |
| 16. | TiO₂-PPy_550 under N₂ | 550 | 110 | 0.90 |
| 17. | TiO ₂ -PPy_600 | 600 | 72 | 0.98 |

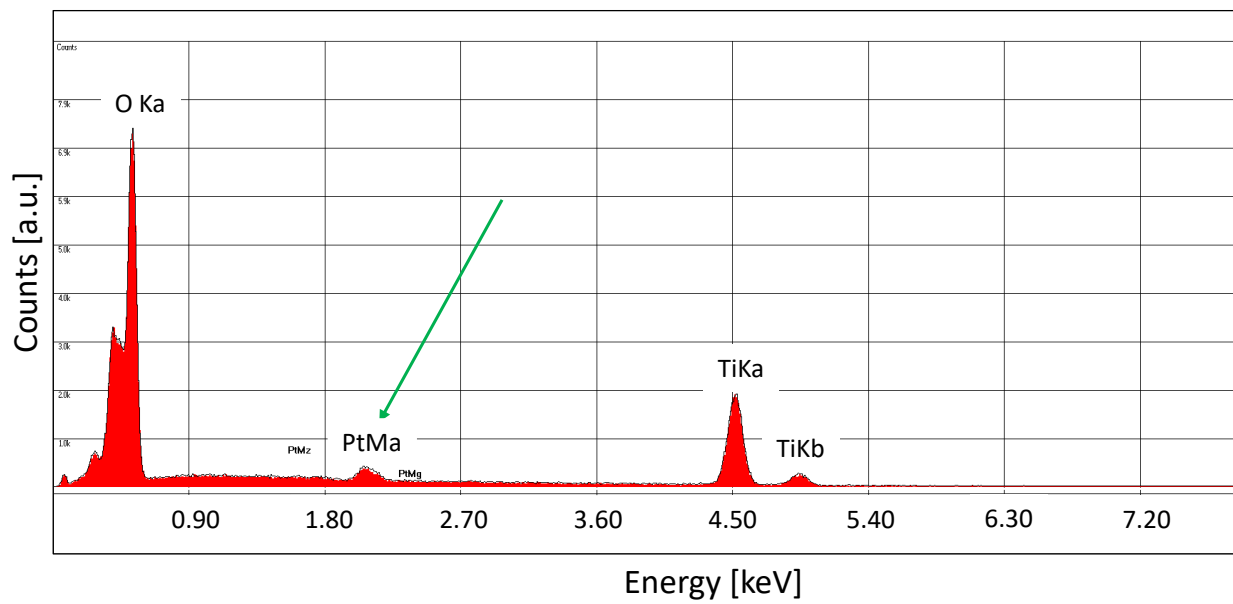


Figure SI 7. EDX analysis confirming the presence of Pt NPs on m-TiO₂.

Setup for the control experiment with Pt NPs only.



Gas chromatograph after the irradiation step with no hydrogen gas detected.

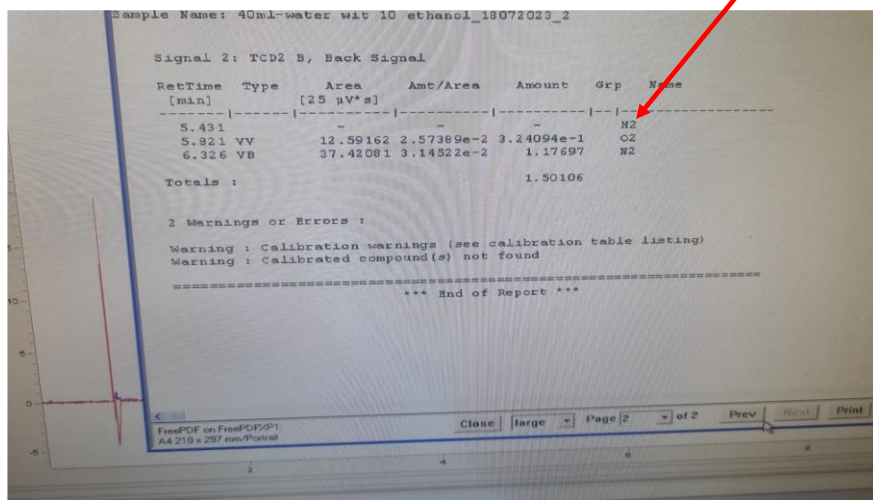


Fig. SI 8 Control experiment using Pt NPs only with irradiation under solar simulation

References

- [1] K. Al-Attafi, A. Nattestad, Q. Wu, Y. Ide, Y. Yamauchi, S.X. Dou, J.H. Kim, Chem. Commun. (Camb), 54 (2018) 381-384, doi:10.1039/c7cc07559f.
- [2] W. Wang, C.-H. Lu, Y.-R. Ni, J.-B. Song, M.-X. Su, Z.-Z. Xu, Catal. Comm., 22 (2012) 19-23, doi:10.1016/j.catcom.2012.02.011.
- [3] Miszczak, S.; Pietrzyk, B., Ceramics International 2015, 41 (6), 7461-7465.
- [4] Z. Ahmad, M.A. Choudhary, A. Mehmood, R. Wakeel, T. Akhtar, M.A. Rafiq, Macromol. Res., 24 (2016) 596-601, doi:10.1007/s13233-016-4081-x.